

Dynamical Crossover and Breakdown of the Stokes–Einstein Relation in Confined Water and in Methanol-Diluted Bulk Water

Francesco Mallamace,^{*,†,‡} Caterina Branca,[†] Carmelo Corsaro,[†] Nancy Leone,[†] Jeroen Spooren,[†] H. Eugene Stanley,[§] and Sow-Hsin Chen[‡]

Dipartimento di Fisica, Università di Messina and IRCCS Neurolesi “Bonino-Pulejo”, I-98166, Messina, Italy; Department of Nuclear Science and Engineering, Massachusetts Institute of Technology, Cambridge, Massachusetts 02139; and Center for Polymer Studies and Department of Physics, Boston University, Boston, Massachusetts 02215

Received: October 20, 2009

Using nuclear magnetic resonance and quasi-elastic neutron scattering spectroscopic techniques, we obtain experimental evidence of a well-defined dynamic crossover temperature T_L in supercooled water. We consider three different geometrical environments: (i) water confined in a nanotube (quasi-one-dimensional water), (ii) water in the first hydration layer of the lysozyme protein (quasi-two-dimensional water), and (iii) water in a mixture with methanol at a methanol molar fraction of $x = 0.22$ (quasi-three-dimensional water). The temperature predicted using a power law approach to analyze the bulk water viscosity in the super-Arrhenius regime defines the fragile-to-strong transition and the Stokes–Einstein relation breakdown recently observed in confined water. Our experiments show that these observed processes are independent of the system dimension d and are instead caused by the onset of an extended hydrogen-bond network that governs the dynamical properties of water as it approaches dynamic arrest.

Introduction

Understanding the properties of water is essential for a wide range of physical and biological processes, and is a key point in many areas of technological development. A number of the thermodynamic and transport properties of liquid water exhibit unusual behavior, especially at low temperatures. In the supercooled regime below the melting point T_M ,^{1–3} the behavior of water seems to indicate that there is a singular temperature at which various thermodynamic response functions and transport properties diverge. Scientists have long sought a coherent explanation for this behavior. A second and related puzzle currently being debated concerns how one determines the vitrification temperature of supercooled water.⁴

Dynamical studies of glass-forming liquids have shown that dramatic changes occur in both the macroscopic transport coefficients (viscosity η and self-diffusion coefficient D_S) and the microscopic structural relaxation time (alpha relaxation time τ) as the temperature is lowered toward the glass transition (GT) temperature T_g . Accordingly, a comprehension of the GT in water has been sought through studying the dynamics of water at the molecular level, which is not yet completely understood.^{5,7,6} Experimental observations indicate that when a liquid is supercooled the viscosity (and the related structural relaxation time) increases until it crystallizes or vitrifies. More precisely, on lowering T by merely a few degrees, the viscosity can increase by more than 10 orders of magnitude, in many cases resulting in the length of time to reach equilibrium surpassing experimental measurement time. Upon supercooling, many liquids exhibit a super-Arrhenius behavior over a large temperature range in such transport parameters as the viscosity and

the inverse of the self-diffusion constant.⁸ Such behavior is classified as *fragile*, in contrast to those of other glass-forming materials that are classified as *strong*⁶ when the viscosity and the inverse of the self-diffusion constant exhibit a pure Arrhenius behavior.

Despite many years of detailed study, the temperature dependence of transport coefficients and structural relaxation times, and their fragile behavior in particular, still remain a hot topic of debate. The manner in which η approaches its value in the glass state (solid state) can, in principle, provide information about the molecular dynamics and structure of the fluid and the nature of the GT. The Arrhenius behavior, $\eta = \eta_0 \exp(E/k_B T)$, is commonly associated with a picture of a single particle hopping over potential barriers of uniform height. On the other hand, the super-Arrhenius behavior described by a Vogel–Fulcher–Tamman (VFT) law $\eta = \eta_0 \exp[B T_0 / (T - T_0)]$, where T_0 (related to the calorimetric T_g) defines the ideal glass transition temperature and the factor B gives a measure of fragility of the system, is rationalized by using a free volume argument.⁹ As $T \rightarrow T_0$ the free volume vanishes and the viscosity is predicted to diverge. Although both approaches have been commonly used to describe experimental data, neither one can be considered, from the theoretical point of view, able to describe the complete viscosity behavior especially in a temperature region where glass forming fluids also show a clear viscoelastic behavior.^{10–12} In this situation, it is necessary to include cooperative effects in the dynamics of complex supercooled fluids, enabling it to take into account the cage and clustering phenomena originating from the strong interparticle interaction and packing constraints.^{11,13,14} It is thus very important to consider the transport properties of these fluids, in the quasi-arrested supercooled states, in terms of molecular models including “self-generated” hopping processes over barriers,¹³ energy landscapes, structural frustration, and the onset of heterogeneous and self-similar structures.^{15–19}

* To whom correspondence should be addressed. E-mail: francesco.mallamace@unime.it.

[†] Università di Messina and IRCCS.

[‡] Massachusetts Institute of Technology.

[§] Boston University.

Very recent mode-coupling theory (MCT) approaches,¹³ and other models like hard sphere,²⁰ spin–spin²¹ and percolation^{9,22} suggest the existence of a transition at which the viscosity appears to diverge as the power law

$$\eta = \eta_0 \left(\frac{T}{T_x} - 1 \right)^\mu \quad (1)$$

with $\mu \cong -2$. Such a power law describes the T -dependence of the viscosity of a very large variety of fluid systems. In the high T regime, this model is better than the super-Arrhenius forms commonly used to describe the temperature dependence of $\eta(T)$.⁸ The universality of the exponent μ is still a subject of current research.²³ Furthermore, after analyzing much experimental data it has been established that the relationship $T_x/T_g \leq 1.2$ exists for *fragile* liquids. The crossover temperature T_x ($T_M > T_x > T_g$) marks the boundary between two types of viscous behavior: power law behavior for $T > T_x$ and Arrhenius behavior for $T < T_x$. This crossover phenomenon is sometimes called a fragile-to-strong dynamic crossover. An extremely significant property of this crossover temperature is that, as the temperature is lowered toward the glass transition temperature, T_x marks the beginning of the decoupling of the self-diffusion constant D_S from the viscosity η (or the structural relaxation time τ). This change of behavior is also referred to as the breakdown of the Stokes–Einstein relation (SER). Below T_x , self-diffusion is enhanced more than would be expected from the SER ($D_S \sim T/\eta$).^{24–27} The temperature of the SER breakdown has been hypothesized, on the basis of computer simulations, to roughly coincide with crossing the Widom line, which is the critical isochore above the critical point in the one-phase region.^{28–30}

The decoupling of the shear viscosity and the self-diffusion coefficients indicates the presence of “dynamical heterogeneities”. This means that the liquid dynamics are dominated by specific heterogeneous structures arising from activated mechanisms in the vicinity of the dynamical arrest transition.^{31–33} The SER breakdown and the dynamical heterogeneities are thus intimately connected. It has been demonstrated that the SER breakdown is an example of the role of dynamical heterogeneities in glass formers.^{34,35} Dynamical heterogeneities have been observed both experimentally and in numerical simulations of supercooled liquids.^{36–39} Molecules in one region of the liquid translate and rotate with several orders of magnitude faster or slower than those in neighboring regions. The spatial extent of these areas is mesoscopic, and the time scale of the slowest domains increases on decreasing T , at least as fast as the system’s relaxation time. Thus dynamical heterogeneities imply also that the slow dynamics of the arrested systems are dominated by fluctuations, and that the sudden increase in the corresponding relaxation times as GT is approached is associated with growing length scales of dynamically correlated regions in space. In the case of water, due to the hydrogen bond network the violation of the SER sets on well above the GT.^{30,40}

Recent studies, utilizing a number of different theoretical approaches and MD simulation, have attempted to more adequately describe the properties of dynamical heterogeneities. In particular, it has been confirmed that the microscopic dynamic in supercooled fluids is dominated by fluctuations.^{32,33} It has also been hypothesized that the difference between strong and fragile liquids lies simply in the strength of fluctuation effects and that strong systems show fluctuation-dominated heterogeneous dynamics in a manner similar to those of fragile systems.⁴¹ The growth of length scales and the sudden increase in relaxation times of supercooled liquids is accompanied, in analogy with

conventional critical phenomena, by scaling behavior in correlation times, dynamic correlation lengths, and susceptibilities. This suggests that the SER breakdown can be described using scaling concepts, and in particular the law $D_S \sim \tau^{-\zeta}$ (or $D_S \sim \eta^{-\zeta}$) where $\zeta = \alpha(T)/\beta(T)$, with α and β being T -dependent scaling exponents of the self-diffusion coefficient and the viscosity, respectively.³⁴

In order to experimentally test the existence of dynamical heterogeneities in water and to understand the physical origin of water’s thermodynamic anomalies, we need to study supercooled liquid water well below its homogeneous nucleation temperature $T_H \approx 231$ K. This is made possible by confining water inside a nanoporous structure so small that the liquid cannot freeze.⁴² Among recent findings concerning water’s dynamical properties at these low temperatures are the following phenomena:

(i) the existence of the water polymorphism for which water is a mixture of two different liquid local structures one corresponding to a low-density liquid (LDL) and the other to a high-density liquid (HDL)⁴³ that supports the liquid–liquid (LL) critical point hypothesis;^{1–3}

(ii) the existence of a density minimum at about 200 K at ambient pressure;^{44,45}

(iii) the presence of a maximum in the thermal expansion coefficient $\partial \ln \rho / \partial T$ and in the specific heat $C_p(T)$;^{44,46} and

(iv) the occurrence of the *fragile-to-strong dynamic* crossover phenomenon (FSC)^{42,47–50} accompanied by the violation of the Stokes–Einstein relation (SER) at and below the FSC temperature.^{28,51}

Phenomena (ii), (iii), and (iv) occur at the same temperature, and thus $T_L = T_x \approx 225$ K and the maxima in $\partial \ln \rho / \partial T$ and $C_p(T)$ provide, for the first time, evidence that the thermodynamical anomalies in water are not the well-known critical-point-like divergences.

These results have received some criticism. For example, it was claimed⁵² that the structural relaxation may not be observed for water confined in nanopores and the fragile-to-strong transition can be due to the vanishing of the cooperative structural relaxation. It has also been suggested that they can be attributed to the geometrical constraints of the confining substrate or to the presence of the interfacial water. In particular, because the nanopores have a cylindrical geometry characterized by a diameter of only tens of angstroms and a length of a few micrometers, one can ask whether these experimental findings pertain only to a form of low-dimensional water. Moreover, it has been suggested that there is a possibility that the steep increase in the relaxation time is not due to the glass transition, but rather due to extra activation energy stemming from low-energy local structures stabilized by hydrogen bonding. Thus, the FSC can be related to a different scenario.⁵³ On considering such a situation and two very recent experimental studies on bulk water confirming the occurrence of the phenomena (i) and (iv),^{40,54} the aim of the present work, by focusing on water confined on a protein surface and a bulk water–methanol mixture (of a precise molar fraction), is to confirm definitively that the observed phenomena, and especially the FSC and the breakdown of the SER, are characteristic properties of water in the supercooled metastable phase, independent of any confining geometry (its dimension) and of any interaction with the confining material surface.

Results and Discussion

We report data on the dynamical parameters of water, the self-diffusion coefficient (D_S), and the average translational

relaxation time $\langle\tau_T\rangle$ (a quantity proportional to the viscosity η)⁴² in the range $280 > T > 190$ K, obtained by nuclear magnetic resonance (NMR)⁴⁹ and quasi-elastic neutron scattering (QENS),⁴² respectively. For confined water we have used a micelle-templated mesoporous silica matrix MCM-41-S, which has quasi-1d cylindrical tubes, with a length of some micrometers, arranged in hexagonal arrays.⁴² This water-confining system is one of the most suitable adsorbent models currently available.⁴⁹ In particular, we have studied fully hydrated MCM-41-S samples with a pore diameter of $\phi = 18$ and 14 Å. The combination of these two experimental methods (NMR and QENS) shows SER breakdown in water. Furthermore, the FSC has been observed for the first time by means of a QENS experiment by studying the $\langle\tau_T\rangle$ temperature behavior.⁴² In fact, as the T is lowered, a $\langle\tau_T\rangle$ versus $1/T$ plot exhibits a cusp-like crossover from non-Arrhenius to Arrhenius behavior at a given temperature T_L . The same technique, used as a function of the pressure, P , reveals a very interesting scenario: the crossover temperature $T_L(P)$ decreases steadily upon increasing P until it intersects the T_H line of bulk water at $P \sim 1.6$ kbar. These results, suggestive of the existence of two liquid phases, have been explained in a molecular dynamics (MD) simulation study by considering the possibility that a second critical point exists. The MD study shows that the FSC line coincides with the line of the specific heat maxima C_p^{\max} (i.e., the Widom line).⁵⁰ Moreover, it is observed that crossing this line corresponds to a change in the T -dependence of both the water dynamics and the structure. More precisely, the calculated water diffusion coefficient, $D_S(T)$, changes according to a FSC, while the structural and thermodynamic properties change from those of the high-density liquid (HDL) to those of low-density liquid (LDL) phase.^{50,43}

In the case of protein we deal with the dynamics of the hydration water in a powder of the globular protein lysozyme. For a hydrated protein, there are two categories of water molecules identifiable in close proximity to the protein: (i) the bound internal water and (ii) the surface water, usually called hydration water. In addition, the bound internal water molecules, located in the internal cavities of the protein, play a structural role in the folded protein itself. It is well-known that the hydration has a strong influence on protein dynamics—demonstrated by experiments and simulations⁵⁵—and on biochemical activity. In lysozyme, enzymatic activity remains very low up to a hydration level h of about 0.2 (h is measured in grams of water per gram of dry protein) then increases sharply when h increases from 0.2 to 0.5.⁵⁶ Proteins also show a sharp slowing down in their functionalities at a transition temperature at about 225 K. Neutron scattering experiments on hydrated lysozyme demonstrate that the origin of this characteristic temperature, which controls both the activity of the protein and the transition in the behavior of the mean-squared atomic displacement $\langle r^2 \rangle$, is the FSC phenomenon in hydration water, which shares the same crossover temperature with the protein.⁵⁷ This neutron study, combined with a Fourier transform infrared (FTIR) experiment on the same system (protein hydration water), indicates that such a dynamic behavior can be ascribed to the hydration water crossing the Widom line,⁵⁸ a result also confirmed by computer simulations.⁵⁹ These experiments used hydration levels of $h = 0.30$, and 0.32 . Hydration level $h = 0.30$ corresponds to a complete first hydration layer, which allows us to explore the SER in the case of water molecules distributed on a globular surface, such as that in a lysozyme protein.

Although all these studies show that the protein glass transition⁶⁰ is connected to the change of local hydrogen bond

patterns of hydration water, the underlying microscopic mechanisms are still to be unveiled. An explanation of this can be obtained by taking into account the “amphiphilic” character of the protein, i.e., the macromolecules have hydrophobic moieties that repel water molecules and hydrophilic moieties that attract them. In this way, a complex HB network is generated. The observation of biological inactivity in anhydrous proteins, as well as the coincidence of the activation temperature of hydrated proteins with the Widom line in water,^{57,59} leads to the conclusion that understanding the interactions between the amphiphilic groups and water is fundamental to the comprehension of biological phenomena.

Aqueous solutions of small amphiphilic molecules can thus be used as model systems to understand such interactions. The simplest amphiphilic molecule is methanol, with the chemical formula CH_3OH , which consists of a single hydrophilic (OH) and a single hydrophobic (CH_3) group. Despite the fact that water and methanol are both relatively simple molecules, the thermodynamic and transport properties that result when they are mixed exhibit a behavior that is much more anomalous than would be expected in an ideal mixture of the pure liquids; e.g., the diffusion coefficient and the excess entropy are considerably smaller, and the viscosity notably larger, indicating strong interactions between the two liquids.^{61–63}

Neutron scattering and MD studies, mainly performed at room temperature, enable us to interpret these phenomena. At low methanol concentration, a slight compressive effect is exerted on the water structure by the methanol molecules. At high methanol concentration, a segregation on the molecular scale takes place (the methyl groups are pushed toward each other and the methanol hydroxyl groups organize themselves around small water clusters).^{62,64,65} MD simulations have also confirmed that water and methanol in solution are not randomly mixed, but form clusters.⁶⁶ For some concentrations, these clusters seem to increase in size and percolate, even when their structures break and reform very rapidly (in the order of picoseconds). To be precise, the peculiar characteristic of water is in the formation, on decreasing temperature, of a well-defined percolating hydrogen bond network.²² In particular, it has been observed⁶⁵ that both water and methanol appear to form separate percolating networks. From these studies, a special structural behavior as a function of the concentration emerges; the value of $x \approx 0.27$ (with x being the methanol molar fraction) determines the approximate alcohol concentration below which water percolates throughout the mixture while methanol does not. For $x > 0.27$ methanol also percolates in the mixture. On increasing the methanol molar fraction, the spanning water percolating cluster becomes increasingly isolated. From these experimental and MD results, there is the indication that, in the concentration range $0.27 < x < 0.54$, both water and methanol clusters percolate simultaneously, making this a bipercolating liquid mixture. The fractal dimension d_f of the water network increases on increasing the water content from 1.89 ($x = 0.54$) to 2.03 ($x = 0.27$), evolving at the lowest methanol concentration toward the values of the volume (3d) random percolation ($d_f = 2.5$).

This could imply that the peculiar dynamical behavior of water–methanol solutions is due to these clustering effects.⁶⁷ In fact, depolarized Rayleigh light scattering, by giving the hydrogen bond relaxation time as a function of temperature and methanol molar fraction, provides evidence that the water–methanol thermodynamic anomalies are due to complex hydrogen bond dynamics (occurring on a picosecond time scale).

Understanding the anomalies of this water–alcohol mixture has been the subject of numerous analyses, one of the earliest being that of Frank and Evans who proposed just a structural origin for its behavior.⁶⁸ In particular, they proposed that the normal water structure is significantly enhanced by the hydrophobic entity, resulting in a more ordered “iceberg-like” structure near the methyl headgroup. It is reasonable to suppose that water on a hydrophobic surface loses hydrogen bonds, causing its enthalpy to increase. In order to compensate for this rise in enthalpy in the vicinity of hydrophobic sites, the local arrangement of water molecules expands to form low-density clusters with a resulting lower entropy.⁶⁸ The folding of proteins is believed to be principally induced by the entropic loss of water molecules around their hydrophobic sites.⁶⁹ Recently, NMR experiments have been performed to measure the spin–lattice T_1 and spin–spin T_2 relaxation times of the three functional groups in water–methanol mixtures at different methanol molar fractions as a function of temperature in the range $205\text{ K} < T < 295\text{ K}$. It has been observed that at all concentrations these relaxation times are, because of strong interactions, faster than those of pure water and methanol, and this results in a complex hydrogen-bonding dynamics that determines their thermodynamic properties. In particular, it has been observed how the interplay between hydrophobicity and hydrophilicity changes with T and influences these relaxations. These results confirm that hydrophobicity at high temperatures creates stable water–methanol clusters in the mixture, and that when the temperature is lowered, tetrabonded water clusters dominate.⁷⁰ Thus, there are in the mixture two different local structures in competition with each other whose populations change with the temperature, a situation that may be at the origin of the heterogeneous dynamics.⁷¹

We performed NMR experiments using a spectrometer operating at 700 MHz ^1H resonance frequency (Bruker AVANCE). The water D_S in all the studied systems was measured with the pulsed gradient spin–echo technique (^1H -PGSE),⁷² in the temperature range 190–298 K; the T dependence of the methanol chemical shift was used as a T standard. All details about the NMR experiment and the sample properties are reported elsewhere;⁴⁹ we stress that the self-diffusion coefficient values were derived from the measured mean square displacement $\langle r^2(t) \rangle$ of molecules diffusing along the NMR pulsed field gradients direction \mathbf{r} , during the time interval t . In the case of the water–methanol mixture, we study separately the D_S of water and methanol molecules by considering the water protons and protons of the hydroxyl (OH) and the methyl (CH_3) groups.

We use high-resolution QENS spectroscopy method to determine the T -dependence of $\langle \tau_T \rangle$ for the confined water and protein hydration water. Because neutrons can easily penetrate the wall of the sample cell and because they are predominantly scattered by hydrogen atoms in water, rather than by the matrices containing it, incoherent QENS is an appropriate tool. The translational relaxation time from 0.2 to 10^4 ps was measured by using two separate high-resolution QENS spectrometers, over the entire temperature range. The experiments were performed at both the high-flux backscattering (HFBS) and the disk-chopper time-of-flight (DCS) spectrometers in the NIST Center for Neutron Research (NIST-NCNR). The two spectrometers used to measure the spectra have two widely different dynamic ranges (for the chosen experimental setup), one with an energy resolution of $0.8\ \mu\text{eV}$ (HFBS) and a dynamic range of $\pm 11\ \mu\text{eV}$,⁷³ and the other one with an energy resolution of $20\ \mu\text{eV}$ (DCS) and a dynamic range of $\pm 5\ \text{meV}$,⁷⁴ in order to be able

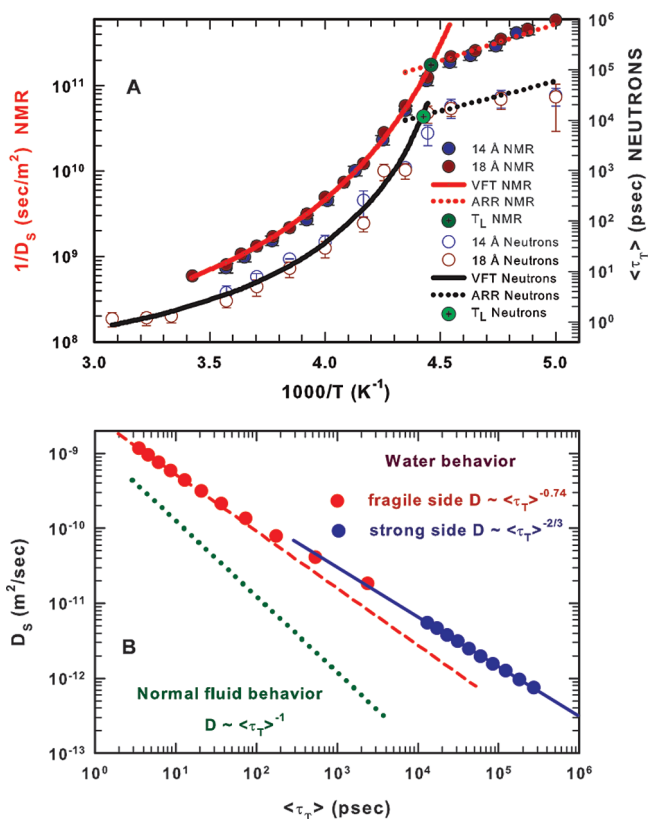


Figure 1. Existence of the FSC and of the SER breakdown in confined water. (A) A log–linear plot of the inverse of the self-diffusion coefficient of water $1/D_S$ measured by NMR (left side)⁴⁹ and the QENS average translational relaxation time $\langle \tau_T \rangle$ (right side)⁴² versus $1/T$, for the fully hydrated MCM-41-S samples with pore diameters of 14 and 18 Å. Note that the measured values of D_S and $\langle \tau_T \rangle$ are independent of the sample pore sizes. The crossover temperature values are about the same, in particular $T_{L1}^{\text{NMR}} = 224 \pm 2\text{ K}$ and $T_{L1}^{\text{QENS}} = 225 \pm 2\text{ K}$. For both the neutron-QENS and NMR data, the solid lines denote the data fit with a VFT relation, whereas the short dotted lines denote the fit to an Arrhenius law. In both fits we have used the same prefactor ($1/D_0$ for NMR and τ_0 for QENS). (B) The log–log scaling plot of D_S vs $\langle \tau_T \rangle$ for MCM confined water.⁵¹ The data fit with a red dashed line correspond to temperatures above T_L , when water is in the super-Arrhenius (fragile) region, whereas the solid blue line corresponds to the strong Arrhenius region. Two different scaling behaviors exist above and below the temperature of the FSC. In the fragile region the scaling exponent is $\zeta \approx 0.74$ (dashed line) and $\approx 2/3$ in the strong region (solid line). The dotted line represents the situation in which the SER holds, namely, $D_S \sim \tau^{-1}$.

to extract the broad range of the relaxation time from the measured spectra. We have used the relaxing-cage model to extract the average translational relaxation time $\langle \tau_T \rangle$.⁴⁸ In the case of water–methanol mixture, just to test the validity of the SER we have used both the measured self-diffusion coefficients D_S and viscosities η as a function of the temperature.⁶³

Figure 1 shows, for both the QENS and NMR data, the existence of the FSC phenomenon (Figure 1A) and the evidence of SER breakdown (Figure 1B) in quasi-1d confined water. In particular, Figure 1A reports, in a log–linear plot, the inverse of the self-diffusion coefficient of water $1/D_S$, measured by NMR (left side), and the average translational relaxation time $\langle \tau_T \rangle$ (right side), measured by QENS, versus $1/T$, for the fully hydrated MCM-41-S samples with pore diameters of 14 and 18 Å.⁴² Figure 1A also shows that the measured values of D_S and $\langle \tau_T \rangle$ are independent of the sample pore sizes.

We analyzed data using the VFT law, $1/D_S = 1/D_0 \exp[BT_0/(T - T_0)]$, for the case of NMR data, in the fragile region; in

Figure 1A the solid lines denote such a fit, whereas in the T region in which the system is a strong glass-forming liquid the data are fitted with an Arrhenius law, $1/D_S = 1/D_0 \exp(E_A/k_B T)$. The dotted lines denote such a fit. In both experiments (NMR and QENS) for both the high- T VFT and low- T Arrhenius data fitting, we used the same prefactor ($1/D_0$ or τ_0) in the formulas. The consequence of using the same prefactor in both the super-Arrhenius and the Arrhenius laws results in an equation determining the crossover temperature T_L in the form

$$\frac{1}{T_L} = \frac{1}{T_0} - \frac{Bk_B}{E_A} \quad (2)$$

Thus, from the NMR fit we obtain $1/D_0 = 2.4 \times 10^7 \text{ s/m}^2$, $B = 1.775$, and $T_0 = 187 \text{ K}$, and in the strong region $E_A = 3.98 \text{ kcal/mol}$. For the neutron $\langle\tau_T\rangle$ data by using the same prefactor $\tau_0 = 0.077 \text{ ps}$ we obtain $E_A = 5.4 \text{ kcal/mol}$, $B = 1.57$, and $T_0 = 200 \text{ K}$. Furthermore, we find that the crossover temperature values are about the same: $T_{L,1}^{\text{NMR}} = 224 \pm 2 \text{ K}$ and $T_{L,1}^{\text{QENS}} = 225 \pm 2 \text{ K}$ (the subscript 1 indicates the system dimensionality, i.e., $d = 1$). The agreement between NMR and QENS results is thus satisfactory, especially regarding T_L ; about the activation energies E_A the difference between the NMR and QENS results is that in the neutron case, we have not considered also the rotodiffusional contributions.⁷⁵ A FSC occurring at $\approx 228 \text{ K}$ has been originally proposed for water,⁴⁷ by observing that water is fragile at room and moderately supercooled temperatures but near the glass transition temperature, as shown by dielectric relaxation measurements, water is a strong liquid.⁷⁵ Whereas a fitting, by using the above-mentioned power law, for the super-Arrhenius temperature region of its viscosity data gives $T_L^{\text{visco}} = 225 \text{ K}$.⁸

Since $\langle\tau_T\rangle$ is proportional to the viscosity, the SER breakdown in confined water is examined by means of D_S and $\langle\tau_T\rangle$, quantities coming out from different experiments and reported on a log–log scale in Figure 1B. We must stress that in the theory of simple liquids the correlation time of the velocity autocorrelation function is directly related to self-diffusion and not to shear viscosity; thus in terms of the simple liquid theory the translational “alpha” relaxation time we extracted from incoherent neutron scattering or NMR experiments is related to the self-diffusion coefficient. But according to mode coupling theory (the extended version proposed by Chong¹³) in a dense liquid, the single particle motion is strongly coupled to the density fluctuation so that both the incoherent and coherent alpha relaxation times can be shown to scale in temperature together nicely with viscosity. The coherent alpha relaxation time is of course legitimately related to the viscosity. To clarify the SER breakdown in terms of the current models on this phenomenon as linked to the dynamical heterogeneities, we use an approach based on scaling concepts, in particular the above-mentioned law $D_S \sim \tau^{-\zeta}$.³⁴ Depending on the fragile or strong glass-forming character of the supercooled liquid, experimental results give different ζ values. It has been shown that for a fragile glass former (trisnaphthylbenzene) $\zeta = 0.77$,³⁷ whereas an MD simulation of Lennard-Jones binary mixture has given $\zeta = 0.75$.⁷⁶ Such results clarify our SER findings for confined supercooled water. In Figure 1B the dashed line represents data corresponding to temperatures above T_L , where water behaves as a fragile glass former, and the continuous line pertains to the strong Arrhenius region. As it can be observed, the data clearly show two different scaling behaviors above and below the FSC temperature, in particular $\zeta \approx 0.74$ on the fragile side

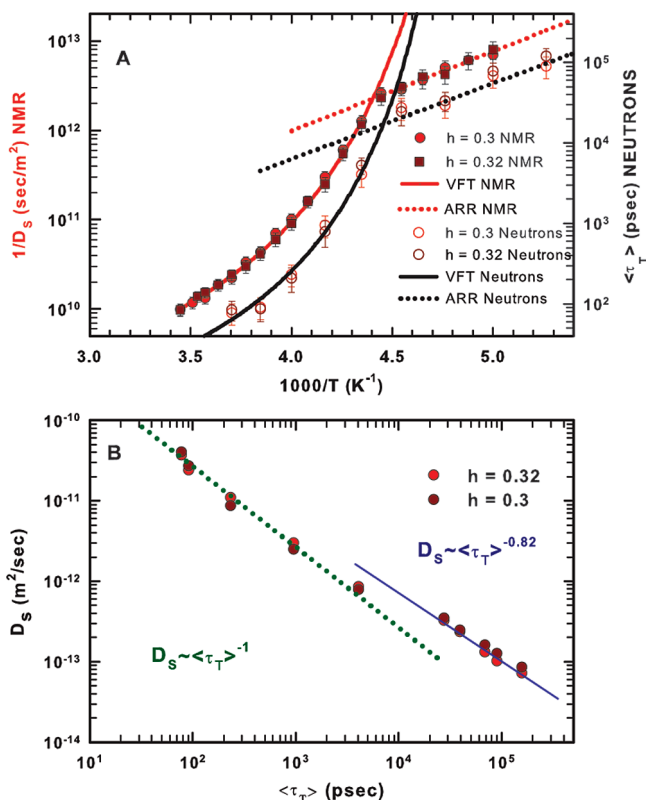


Figure 2. Existence of (A) the FSC and (B) the SER breakdown in the case of the lysozyme hydration water with hydration levels of $h = 0.30$ ⁵⁸ and $h = 0.32$. Part A reports the NMR $1/D_S$ in a log–lin plot (left side) and the QENS average translational relaxation time $\langle\tau_T\rangle$ (right side) vs $1/T$. The obtained crossover temperatures are $T_{L,2}^{\text{NMR}} = 226 \pm 2 \text{ K}$ and $T_{L,2}^{\text{QENS}} = 225 \pm 2 \text{ K}$. Part B reports the analysis of the scaled SER, a log–log plot of D_S vs $\langle\tau_T\rangle$ for both hydration levels. There are two scaling behaviors above and below T_L : in the super-Arrhenius region we have $\zeta \approx 1$, whereas in the Arrhenius region $\zeta \approx 0.82$, the value predicted by theory and numerical analysis for a quasi-2d system.

(dashed line) and $\zeta \approx 2/3$ on the strong side (solid line). The dotted line represents the situation in which the SER holds, namely, $D_S \sim \tau^{-1}$. These results agree with those obtained in trisnaphthylbenzene.³⁷ More specifically, they agree with results of a recent theoretical study in which the decoupling of transport coefficients in supercooled liquids was investigated by using two classes of models, one describing diffusion in a strong glass former, and the other in a fragile one.³⁴ The main result of this study is that, while in the fragile case the SER violation is weakly dependent on the dimensionality d , with $\zeta = 0.73$, in the strong case the violation is sensitive to d , going as $D_S \sim \tau^{-2/3}$ for $d = 1$, $D_S \sim \tau^{-2/2.3}$ for $d = 2$ and as $D_S \sim \tau^{-0.95}$ for $d = 3$. On considering the geometry of the system that we have used in our experiment to confine water (quasi-1d cylindrical tubes, with a length of some micrometers and pore diameters of $\phi = 14$ and 18 \AA), the scalings shown in Figure 1B agree remarkably well with the findings of the theoretical predictions,³⁴ on both the fragile and strong sides.

Figure 2 deals with the results obtained in the case of the lysozyme hydration water with hydration levels of $h = 0.30$ ⁵⁸ and $h = 0.32$, corresponding to a complete first hydration layer of water around the protein, a situation that gives us the possibility to explore both the existence of the FSC and the validity of the SER in the case of water molecules distributed on a globular protein surface (i.e., $d = 2$). We show in Figure 2A the NMR ($1/D_S$) and QENS ($\langle\tau_T\rangle$) data plotted in a log–lin

scale as a function of $1/T$. The data analysis is the same as in the case of quasi-1d confined water (water in MCM-41-S). Results obtained for the significant quantities are the following: in the NMR case from the data-fitting we obtain $1/D_0 = 2.7 \times 10^8 \text{ s/m}^2$, $B = 2.05$, and $T_0 = 185 \text{ K}$, and in the strong region $E_A = 4.07 \text{ kcal/mol}$; whereas for the neutron data we have $E_A = 4.31 \text{ kcal/mol}$ and $T_0 = 191 \text{ K}$. The obtained crossover temperatures are $T_{L,2}^{\text{NMR}} = 226 \pm 2 \text{ K}$ and $T_{L,2}^{\text{QENS}} = 225 \pm 2 \text{ K}$. We have to stress that in this case the crossover temperatures are nearly the same as those found in nanopore confined water; i.e., T_L for confined water is independent of the dimensionality of the confining geometry. Figure 2B gives the result of analysis in terms of the scaled SER, i.e., a log–log plot of D_S vs $\langle\tau_T\rangle$, for both the above-mentioned lysozyme hydration levels. Note that we find two scaling behaviors, above and below T_L . More precisely in the super-Arrhenius region we have $\zeta \approx 1$, whereas in the strong Arrhenius supercooled temperature region $\zeta \approx 0.82$ a value very close to $2/2.3$, i.e., the value predicted by theory and numerical analysis for a quasi-2d system.³⁴ These latter results give a proof that the dynamical heterogeneities, and thus the hydrogen-bonding network, have the same effects for quasi-1d and quasi-2d systems. Hence it may be useful to test whether such a situation holds also for 3d systems. The main criticism for the FSC and SER breakdown results in MCM-41-S quasi-1d cylindrical samples was that these phenomena are characteristic of a confined water (presumably due to the interfacial water, i.e. the water layer in proximity of the solid substrate material). Therefore, one needs to demonstrate that these properties genuinely belong to the bulk water. Thus an analysis made in a bulk water–methanol mixture with a substantial amount of water molecules, with respect to methanol can help us to clarify such a situation. For this reason we have considered a water–methanol mixture with a methanol molar fraction of $x = 0.22$ (i.e., about 4 water molecules per methanol molecule). At this concentration in which neutron and MD experiments⁶⁵ clearly indicate that water is arranged in volume percolating clusters. Such a concentration also allows us to reach a temperature of about 210 K, i.e. well below the water crossover temperature T_L , maintaining water in the liquid phase and in a bulk situation. The aim is thus to give definitive information that the crossover temperature may be independent of the system dimension as our experiments in quasi-1d and quasi-2d systems seem to suggest. Such a hypothesis is of deep and broad interest, because if true, dynamical heterogeneities, and thus the hydrogen bonding network, drive at the same way properties of bulk and confined water. Thus, one can explain processes on the borderline between physics and biology, as biological matter is composed mainly of confined water (e.g., water in cells, water in tissue, water in the brain, etc.).

Figure 3 reports the NMR D_S values vs $1/T$ measured in bulk methanol,⁷⁷ and water in the water–methanol mixture for $x = 0.22$; for comparison are reported the data measured in bulk water⁷⁸ and in the MCM-41-S sample.⁴⁹ As it can be observed, the methanol self-diffusion data present a moderately super-Arrhenius behavior in the entire temperature range studied, whereas water in the methanol mixture and confined water in MCM-41-S have an analogous $1/T$ behavior: super-Arrhenius in the high-temperature region and Arrhenius at the lowest T ; both data show a marked crossover at about the same temperature. It must be also noticed that at higher T the water self-diffusion in the solution is slightly smaller than that of water, whereas in the low-temperature regime it is higher than that of confined water. The T at which these D_S values overlap is about 250 K, the same one in which the measured NMR spin–lattice

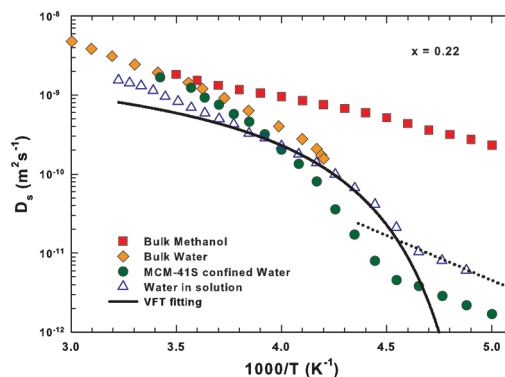


Figure 3. D_S vs $1/T$ measured in the water–methanol mixture for $x = 0.22$. For comparison the data measured in bulk water⁷⁸ and in bulk methanol,⁷⁷ and water in the MCM-41-S sample⁴⁹ are reported. The methanol self-diffusion presents a moderately super-Arrhenius behavior in the whole studied T range, whereas water in the methanol mixture and confined in MCM have an analogous $1/T$ behavior: super-Arrhenius in the high-temperature region and Arrhenius at the lower reported T ; both show a marked crossover at about the same temperature. In fact, we obtain from the fit of the water–methanol mixture D_S data: $T_{L,3}^{\text{NMR}} = 223 \pm 2 \text{ K}$.

T_1 and spin–spin T_2 relaxation times evidence the change in the clustering processes dominated by hydrophobicity ($T > 250 \text{ K}$) and hydrophilicity ($T < 250 \text{ K}$).⁷⁰

The VFT fit of these data gives $1/D_0 = 3.73 \times 10^8 \text{ s/m}^2$, $B = 0.7275$, and $T_0 = 192 \text{ K}$, whereas in the Arrhenius region we calculate $E_A = 4.28 \text{ kcal/mol}$. The fitting gives also $T_{L,3}^{\text{NMR}} = 223 \pm 2 \text{ K}$. Note that for the data fit in the super-Arrhenius region we consider, as is evident from Figure 3, only the self-diffusion values in the temperature region $T < 250 \text{ K}$. The reason lies in the fact that we must consider the results obtained, for the same system, from the NMR relaxation times T_1 and T_2 , for which below 250 K, the system properties are dominated only by the tetrabonded water clusters without the influence of the methanol hydrophobic groups. The crossover temperature is about the same for all three considered cases, and so is independent of the dimensionality of the water host. Such a result suggests that the FSC is entirely due to the onset of the water hydrogen bond network.^{44,71} Before discussing this important point we observe that Figure 4 reports the SER breakdown in two separate ways: a plot of $D_S\eta/T$ vs T (Figure 4A) and in the scaling representation as a log–log of D_S vs η (Figure 4B). Figure 4A reports the quantity $D_S\eta/T$ as a function of T (in the range $200 < T < 300 \text{ K}$) for bulk water, bulk methanol, water in the actual water–methanol solution ($x = 0.22$), water confined in MCM-41 quasi-1d nanotubes, and protein hydration water. The $D_S\eta/T$ values for these latter two systems are properly scaled, being calculated by considering instead of the viscosity η (actual case) the average longitudinal relaxation time $\langle\tau_T\rangle$. Note that only water systems show a clear SER breakdown at about the same crossover temperature $T_L \approx 225 \text{ K}$, whereas the pure methanol remains for all the investigated T range nearly constant. For bulk water are available D_S ⁷⁸ and η ⁷⁹ data only for $T > 243 \text{ K}$. Figure 4B shows in the scaling plot D_S vs η data coming out from bulk methanol, bulk water and water in the actual studied solution. We see that pure bulk methanol and pure bulk water fall in a region of validity of the SER ($\zeta \approx 1$, solid line), whereas the water–methanol solution with $x = 0.22$ data clearly show two different scaling behaviors above and below the FSC temperature. In particular, $\zeta \approx 1$ on the fragile side (solid line) and $\zeta \approx 0.9$ on the strong side (dotted line). This latter measured value of the exponent $\zeta \approx 0.9$ agrees well with the value theoretically proposed for a 3-d glass

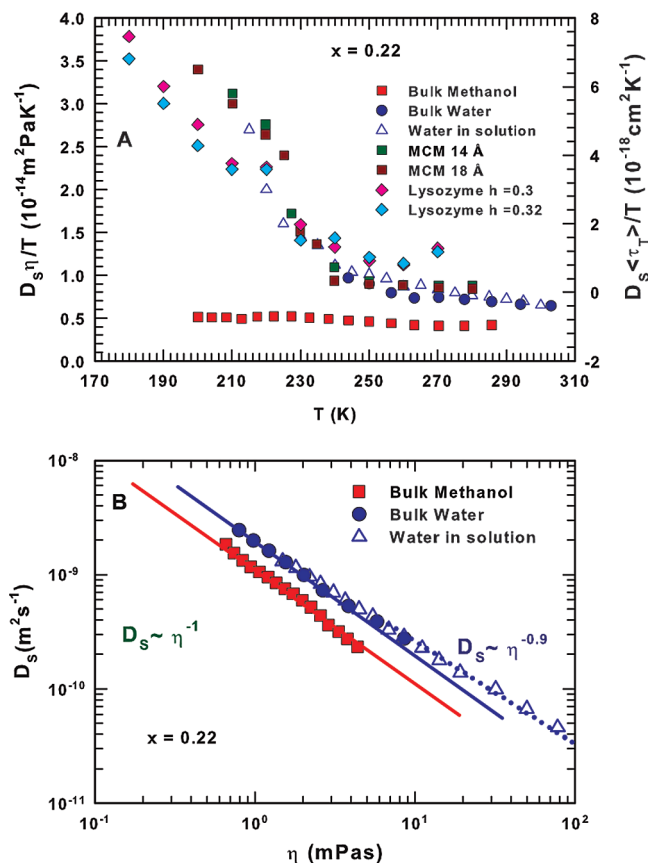


Figure 4. Water SER breakdown reported as (A) $D_s \eta / T$ vs T and (B) in the scaling representation as a log–log of D_s vs η . Part A shows, as a function of T , the quantity $D_s \eta / T$ for bulk water, bulk methanol, water in the actual water–methanol solution ($x = 0.22$) on the left side, and the quantity $D_s \langle \tau_T \rangle / T$ for water confined in MCM quasi-1d nanotubes and the protein hydration water (properly scaled) on the right side. Only water systems evidence a clear SER breakdown at about the same crossover temperature $T_L \approx 225$ K, whereas the pure methanol remains nearly constant for all the investigated T range. Part B shows D_s vs η in the scaling plot for bulk methanol,^{8,77} bulk water,^{78,79} and water in the actual studied solution. For bulk methanol and bulk water in the studied region the SER is valid ($\zeta \approx 1$, solid line), whereas for the water–methanol solution with $x = 0.22$ it takes on two different scaling behaviors above and below the FSC temperature, in particular $\zeta \approx 1$ on the fragile side (solid line) and $\zeta \approx 0.9$ on the strong side (dotted line). This latter measured value of the exponent $\zeta \approx 0.9$ agrees well with the theoretically proposed value for a 3d glass-forming liquid.³⁴

forming liquid.³⁴ A common result of our analysis is that, for all the three different dimensions in which we have considered water, the crossover temperature T_L of the FSC is the same within the experimental error: $T_L \approx 225$ K. Although we have studied pure bulk methanol for the same temperature range as water, we do not observe the FSC and a corresponding crossover temperature (Figure 4A,B). For a proper explanation of both these results, it is useful to consider the power law approach proposed some time ago to study the viscosity behavior of super-Arrhenius fluids. An approach that defines the crossover temperature T_x (or T_L).⁸ Figure 5 shows an analysis of the viscosities of pure bulk methanol and water made by using the previous mentioned power law model, $\eta = \eta_0 (T/T_L - 1)^\mu$. Here we report the quantity $(\eta/\eta_0)^{1/\mu}$ as a function of T/T_L . In such a plot we consider all the available viscosity values in the temperature range in which both the fluids are in the liquid state, i.e., from the metastable supercooled region to the thermodynamically stable phase. However, contrary to the VFT model used to fit the data with an aim to obtain the value of the ideal

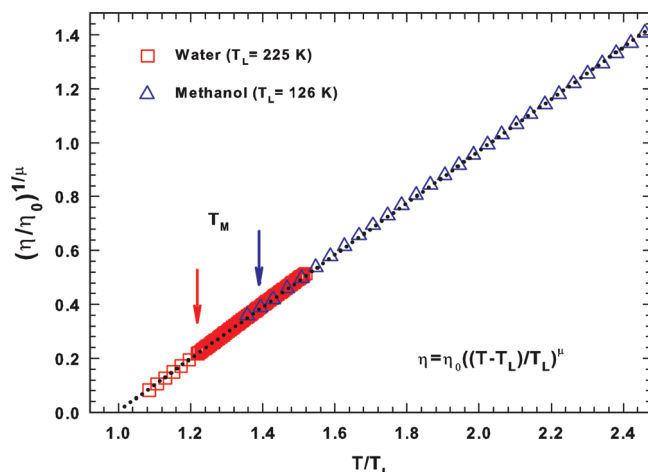


Figure 5. Scaled viscosities $(\eta/\eta_0)^{1/\mu}$ as a function of T/T_L of bulk water⁷⁹ and methanol.⁸ This plot considers for the viscosity of these two liquids the power law approach, $\eta = \eta_0 [(T - T_L)/T_L]^\mu$, which gives $T_L = 225$ K, $\mu = -1.81$ for water, and $T_L = 126$ K, $\mu = -2.16$ for methanol. The colored arrows indicate the melting temperature of the two liquids.

glass transition temperature T_0 , we have used the power law form to fit the experimental $\eta(T)$ data by assuming that the “nonuniversal” exponent μ ranges in the interval -2 ± 0.2 .^{8,23} We obtain $T_L = 225$ and 126 K for water and methanol, respectively, whereas we find $\mu = -1.81$ for water (a value slightly different from the one measured for the isothermal compressibility⁸⁰) and $\mu = -2.16$ for methanol.

The crossover temperature ($T_L = 225$ K) value we obtain in this way for bulk water is interesting because it is the same as that obtained (for confined water in all the dimensions studied here) by means of different transport parameters like D_s and $\langle \tau_T \rangle$ used to verify the existence of the FSC, the SER breakdown, and the onset of the dynamical heterogeneities. It is surprising that such a power law approach, which defines the existence of T_L , is also able to give its exact value by merely using viscosity data that are located in a temperature range far from the region where T_L lies. This suggests that the power law approach may have a larger temperature range of validity compared to the VFT model approach for studying a wide range of supercooled glass forming liquids.

Conclusions

We have considered the dynamical parameters such as the self-diffusion constant, the translational relaxation time, and the shear viscosity of water confined in different environments with different effective dimensions. Our purpose is to verify that recently observed important phenomena, taking place in deeply supercooled regime, such as the FSC and the violation of SER, are the consequence of a transition to more open hydrogen bond network structure. We observe from these physical phenomena, detected separately by means of different experimental techniques, that these processes are independent of the dimension of the water hosting structure and thus are due only to the characteristic properties of water. In particular, we observe that the FSC and the SER violation occur, in all the studied systems, at the same crossover temperature $T_L \approx 225$ K. According to recent theoretical models of water and MD simulations,^{32–36} this is a temperature at which a supercooled glass-forming fluid is characterized by the onset of dynamical heterogeneities. Dynamical heterogeneities are mesoscopic heterogeneous structures generated by density fluctuations that are also origin of the

decoupling of the two transport coefficients as seen in the breakdown of SER.

Another result coming out from our analysis described above is worth stressing. Below the crossover temperature T_L , where the quantities D_S , $\langle\tau_T\rangle$, and η grow many orders of magnitude for a relatively small change of temperature, the same quantities are related to each other, according to the theory, by a scaling law $D_S \sim \tau^{-\zeta}$ (or $D_S \sim \eta^{-\zeta}$). The exponent ζ depends both on temperature and on the dimensionality $d = 1, 2, 3$ of the system.³⁴ We note that our ζ values agree well, within the experimental errors, with those predicted by theory.

Finally, using a power law approach, instead of the VFT equation, to fit the viscosity data in the high-temperature regime, one can define well the crossover temperature T_L for both water and methanol (Figure 5). Such an approach is surprising and deserves attention by people working in glass transition phenomena. If its universality is confirmed definitively,^{8,23} it may influence the way researchers study dynamically arrested matter and jamming phenomena.

Acknowledgment. The authors thank Chun-Wan Yen from National Taiwan University for preparing the MCM-41-S samples. Technical support in QENS measurements from E. Mamontov and J. R. D. Copley at NIST NCNR are greatly appreciated. The research at MIT is supported by DOE Grants DE-FG02-90ER45429 and 2113-MIT-DOE-591. The research at BU is supported by NSF Chemistry Division. The research in Messina is supported by the PRA-Unime-2005. This work utilized facilities supported in part by the National Science Foundation under Agreement No. DMR-0086210. The work utilized facilities of the Messina SCM-HR-NMR Center of CNR-INFN. We benefited from affiliation with EU Marie Curie Research and Training Network on Arrested Matter.

Note Added after ASAP Publication. This paper was published ASAP on January 8, 2010. The Acknowledgment section and ref 22 were revised. The updated paper was reposted on January 13, 2010.

References and Notes

- Mallamace, F. *Proc. Natl. Acad. Sci. U.S.A.* **2009**, *106*, 15097.
- Debenedetti, P. G.; Stanley, H. E. *Phys. Today* **2003**, *56*, 40.
- Mishima, O.; Stanley, H. E. *Nature* **1998**, *396*, 329.
- Velikov, V.; Borick, S.; Angell, C. A. *Science* **2001**, *294*, 2335.
- Sokolov, A. P. *Science* **1996**, *273*, 1675.
- (a) Angell, C. A. *Complex Behavior of Glassy Systems*; Rubí, M., Péres-Vicente, C., Eds.; Springer: Berlin, 1997. (b) Angell, C. A. *Science* **1995**, *267*, 1924.
- Götze, W.; Sjölander, L. *Rep. Prog. Phys.* **1992**, *55*, 241.
- Taborek, P.; Kleinman, R. N.; Bishop, D. J. *Phys. Rev. B* **1986**, *34*, 1835.
- Grest, G. S.; Cohen, M. H. *Adv. Chem. Phys.* **1981**, *48*, 455.
- Miyazaki, K.; Wyss, H. M.; Weitz, D. A.; Reichman, D. R. *Europhys. Lett.* **2006**, *75*, 915.
- (a) Mallamace, F.; Chen, S.-H.; Coniglio, A.; de Arcangelis, L.; Del Gado, E.; Fierro, A. *Phys. Rev. E* **2006**, *73*, 020402(R). (b) Mallamace, F.; Tartaglia, P.; Chen, W. R.; Faraone, A.; Chen, S.-H. *J. Phys.: Condens. Matter* **2004**, *16*, S4975.
- (a) Weeks, E. R.; Crocker, J. C.; Levitt, A. C.; Schofield, A.; Weitz, D. A. *Science* **2000**, *287*, 627. (b) Weeks, E. R.; Weitz, D. A. *Phys. Rev. Lett.* **2002**, *89*, 095704.
- Chong, S. H. *Phys. Rev. E* **2008**, *78*, 041501.
- Goldstein, M. J. *Chem. Phys.* **1969**, *51*, 3728.
- Stillinger, F. H. *J. Chem. Phys.* **1988**, *89*, 6461.
- Kivelson, D.; Tarjus, J. J. *Non-Cryst. Solids* **1998**, *235–237*, 86.
- Havlin, S.; ben-Avraham, D. *Adv. Phys.* **1987**, *36*, 695.
- Ngai, K. L. *J. Non-Cryst. Solids* **1996**, *203*, 232.
- Sillescu, H. *J. Non-Cryst. Solids* **1999**, *243*, 81.
- (a) Leutheusser, E. *Phys. Rev. A* **1984**, *29*, 2765. (b) Bengtzelius, U.; Götze, W.; Sjölander, A. *J. Phys. C: Solid State Phys.* **1984**, *17*, 5915.
- Fredricson, G. H.; Andersen, H. C. *Phys. Rev. Lett.* **1984**, *53*, 1244.
- (22) (a) Stanley, H. E. *J. Phys. A* **1979**, *12*, L329. (b) Stanley, H. E.; Teixeira, J. *J. Chem. Phys.* **1980**, *73*, 3404.
- Elmatad, Y. S.; Chandler, D.; Garrahan, J. P. [cond-mat.stat-mech] **2008**, arXiv:0811.2450v1.
- Stillinger, F. H.; Hodgdon, J. A. *Phys. Rev. E* **1994**, *50*, 2064.
- Tarjus, G.; Kivelson, D. *J. Chem. Phys.* **1995**, *103*, 3071.
- Liu, C. Z.-W.; Hoppenheim, I. *Phys. Rev. E* **1996**, *53*, 799.
- Xia, X.; Wolynes, P. G. *J. Chem. Phys.* **2001**, *105*, 6570.
- Kumar, P.; Buldyrev, S. V.; Becker, S. L.; Poole, P. H.; Starr, F. W.; Stanley, H. E. *Proc. Natl. Acad. Sci. U.S.A.* **2007**, *104*, 9575.
- Mazza, M. G.; Giovambattista, N.; Stanley, H. E.; Starr, F. W. *Phys. Rev. E* **2007**, *76*, 031202.
- Xu, L.; Mallamace, F.; Starr, F. W.; Yan, Z.; Buldyrev, S. V.; Stanley, H. E. *Nat. Phys.* **2009**, *5*, 565.
- Palmer, R. G.; Stein, D. L.; Abrahams, E.; Anderson, P. W. *Phys. Rev. Lett.* **1984**, *53*, 958.
- Garrahan, J. P.; Chandler, D. *Phys. Rev. Lett.* **2002**, *89*, 035704.
- Garrahan, J. P.; Chandler, D. *Proc. Natl. Acad. Sci. U.S.A.* **2003**, *100*, 9710.
- (34) (a) Jung, Y.-J.; Garrahan, J. P.; Chandler, D. *Phys. Rev. E* **2004**, *69*, 061205. (b) Jung, Y.-J.; Garrahan, J. P.; Chandler, D. *J. Chem. Phys.* **2005**, *123*, 084509.
- Pan, A. C.; Garrahan, J. P.; Chandler, D. *Chem. Phys. Chem.* **2005**, *6*, 1783.
- (36) (a) Ediger, M. D. *Annu. Rev. Phys. Chem.* **2000**, *51*, 99. (b) Cicerone, M. T.; Ediger, M. D. *J. Chem. Phys.* **1996**, *104*, 7210.
- Swallen, S. F.; Bonvallet, P. A.; McMahon, R. J.; Ediger, M. D. *Phys. Rev. Lett.* **2003**, *90*, 015901.
- Chang, J.; Sillescu, H. *J. Phys. Chem. B* **1997**, *101*, 8794.
- Ngai, K. L.; Magill, J. H.; Plazek, D. J. *J. Chem. Phys.* **2000**, *112*, 1887.
- Huang, C.; Wikfeldt, K. T.; Tokushima, T.; Nordlund, D.; Harada, Y.; Bergmann, U.; Niebuhr, M.; Weiss, T. M.; Horikawa, Y.; Leetmaa, M.; Ljungberg, M. P.; Takahashi, O.; Lenz, A.; Ojamäe, L.; Lyubartsev, A. P.; Shin, S.; Pettersson, L. G. M.; Nilsson, A. *Proc. Natl. Acad. Sci. U.S.A.* **2009**, *106*, 15214.
- Whitelam, S.; Berthier, L.; Garrahan, J. P. *Phys. Rev. E* **2005**, *71*, 026128.
- Faraone, A.; Liu, L.; Mou, C.-Y.; Yen, C.-W.; Chen, S.-H. *J. Chem. Phys. (Rapid Commun.)* **2004**, *121*, 10843.
- Mallamace, F.; Broccio, M.; Corsaro, C.; Faraone, A.; Majolino, D.; Venuiti, V.; Liu, L.; Mou, C.-Y.; Chen, S.-H. *Proc. Natl. Acad. Sci. U.S.A.* **2007**, *104*, 424.
- Mallamace, F.; Branca, C.; Corsaro, C.; Broccio, M.; Mou, C.-Y.; Chen, S.-H. *Proc. Natl. Acad. Sci. U.S.A.* **2007**, *104*, 18387.
- Liu, D.; Zhang, Y.; Chen, C. C.; Mou, C.-Y.; Poole, P. H.; Chen, S.-H. *Proc. Natl. Acad. Sci. U.S.A.* **2007**, *104*, 9570.
- Mallamace, F.; Corsaro, C.; Broccio, M.; Branca, C.; Gonzalez-Segredo, N.; Spooren, J.; Chen, S.-H.; Stanley, H. E. *Proc. Natl. Acad. Sci. U.S.A.* **2008**, *105*, 12725.
- Ito, K.; Moynihan, C. T.; Angell, C. A. *Nature* **1999**, *398*, 492.
- Liu, L.; Chen, S.-H.; Faraone, A.; Yen, C. W.; Mou, C.-Y. *Phys. Rev. Lett.* **2005**, *95*, 117802.
- Mallamace, F.; Broccio, M.; Corsaro, C.; Faraone, A.; Wanderlingh, U.; Liu, L.; Mou, C.-Y.; Chen, S.-H. *J. Chem. Phys.* **2006**, *124*, 161102.
- Xu, L.; Kumar, P.; Buldyrev, S. V.; Chen, S.-H.; Poole, P. H.; Sciortino, F.; Stanley, H. E. *Proc. Natl. Acad. Sci. U.S.A.* **2005**, *102*, 16558.
- Chen, S.-H.; Mallamace, F.; Mou, C.-Y.; Broccio, M.; Corsaro, C.; Faraone, A.; Liu, L. *Proc. Natl. Acad. Sci. U.S.A.* **2006**, *104*, 12974.
- Hedstrom, J.; Swenson, J.; Bergman, R.; Jansson, H.; Kittaka, S. *Eur. Phys. J. Spec. Top.* **2007**, *141*, 53.
- Tanaka, H. *J. Phys.: Condens. Matter* **2003**, *15*, L703.
- Banerjee, D.; Bhat, S. N.; Bhat, S. V.; Leporini, D. *Proc. Natl. Acad. Sci. U.S.A.* **2009**, *106*, 11448.
- Tarek, M.; Tobias, D. J. *Phys. Rev. Lett.* **2002**, *89*, 275501.
- Roth, J. H.; Novikov, V. N.; Gregory, R. B.; Curtis, J. E.; Chowdhuri, E.; Sokolov, A. P. *Phys. Rev. Lett.* **2005**, *95*, 038101.
- Chen, S.-H.; Liu, L.; Fratini, E.; Baglioni, P.; Faraone, A.; Mamantov, E. *Proc. Natl. Acad. Sci. U.S.A.* **2006**, *103*, 9016.
- Mallamace, F.; Chen, S.-H.; Broccio, M.; Corsaro, C.; Crupi, V.; Majolino, D.; Venuiti, V.; Baglioni, P.; Fratini, E.; Vannucci, C.; Stanley, H. E. *J. Chem. Phys.* **2007**, *127*, 045104.
- Kumar, P.; Yan, Z.; Xu, L.; Mazza, M. G.; Buldyrev, S. V.; Chen, S.-H.; Sastry, S.; Stanley, H. E. *Phys. Rev. Lett.* **2006**, *97*, 177802.
- (60) (a) Vitkup, D.; Ringe, D.; Petsko, G. A.; Karplus, M. *Nat. Struct. Biol.* **2000**, *7*, 34. (b) Doster, W.; Cusack, S.; Petry, W. *Nature* **1989**, *337*, 754.
- Derlacki, Z. J.; Easteal, A.; Edge, A. V. J.; Woolf, L. A.; Roksandic, Z. *J. Phys. Chem.* **1985**, *89*, 5318.
- Soper, A. K.; Dougan, L.; Crain, J.; Finney, J. L. *J. Phys. Chem. B* **2006**, *110*, 3472.

- (63) (a) Mikhail, S. Z.; Kimel, W. R. *J. Chem. Eng. Data* **1961**, *6*, 533. (b) Yergovich, T. W.; Swift, G. W.; Kurata, F. *J. Chem. Eng. Data* **1971**, *16*, 222.
- (64) Dougan, L.; Bates, S. P.; Hargreaves, R.; Fox, J. P.; Crain, J.; Finney, J. L.; Reat, V.; Soper, A. K. *J. Chem. Phys.* **2004**, *121*, 6456.
- (65) Dougan, L.; Hargreaves, R.; Bates, S. P.; Finney, J. L.; Reat, V.; Soper, A. K.; Crain, J. *J. Chem. Phys.* **2005**, *122*, 174514.
- (66) Allison, S. K.; Fox, J. P.; Hargreaves, R.; Bates, S. P. *Phys. Rev. B* **2005**, *71*, 024201.
- (67) Micali, N.; Trusso, S.; Vasi, C.; Blaudez, D.; Mallamace, F. *Phys. Rev. E* **1996**, *54*, 1720.
- (68) Frank, S. H.; Evans, M. W. *J. Chem. Phys.* **1945**, *13*, 507.
- (69) Kauzmann, W. *Adv. Protein Chem.* **1959**, *14*, 1.
- (70) Corsaro, C.; Spooen, J.; Branca, C.; Leone, N.; Broccio, M.; Kim, C.; Chen, S.-H.; Stanley, H. E.; Mallamace, F. *J. Phys. Chem. B* **2008**, *112*, 10449.
- (71) Jana, B.; Bagchi, B. *J. Phys. Chem. B* **2009**, *113*, 2221.
- (72) (a) Stejskal, E. O.; Tanner, J. E. *J. Chem. Phys.* **1964**, *42*, 288. (b) Price, W. S. *Concepts Magn. Reson.* **1998**, *10*, 197.
- (73) Meyer, A.; Dimeo, R. M.; Gehring, P. M.; Neumann, D. A. *Rev. Sci. Instrum.* **2003**, *74*, 2759.
- (74) Copley, J. R. D.; Cook, J. C. *Chem. Phys.* **2003**, *292*, 477.
- (75) Bergman, R.; Swenson, J. *Nature* **2000**, *403*, 283.
- (76) Yamamoto, R.; Onuki, A. *Phys. Rev. Lett.* **1998**, *81*, 4915.
- (77) Karger, N.; Vardag, T.; Lüdemann, H.-D. *J. Chem. Phys.* **1990**, *93*, 3437.
- (78) Price, S. W.; Hiroyudi, I.; Arata, Y. *J. Phys. Chem. A* **1999**, *103*, 448.
- (79) Cho, C. H.; Urquidi, J.; Singh, S.; Wilse Robinson, G. *J. Phys. Chem. B* **1999**, *103*, 1991.
- (80) Speedy, R.; Angell, C. A. *J. Chem. Phys.* **1976**, *65*, 851.

JP910038J